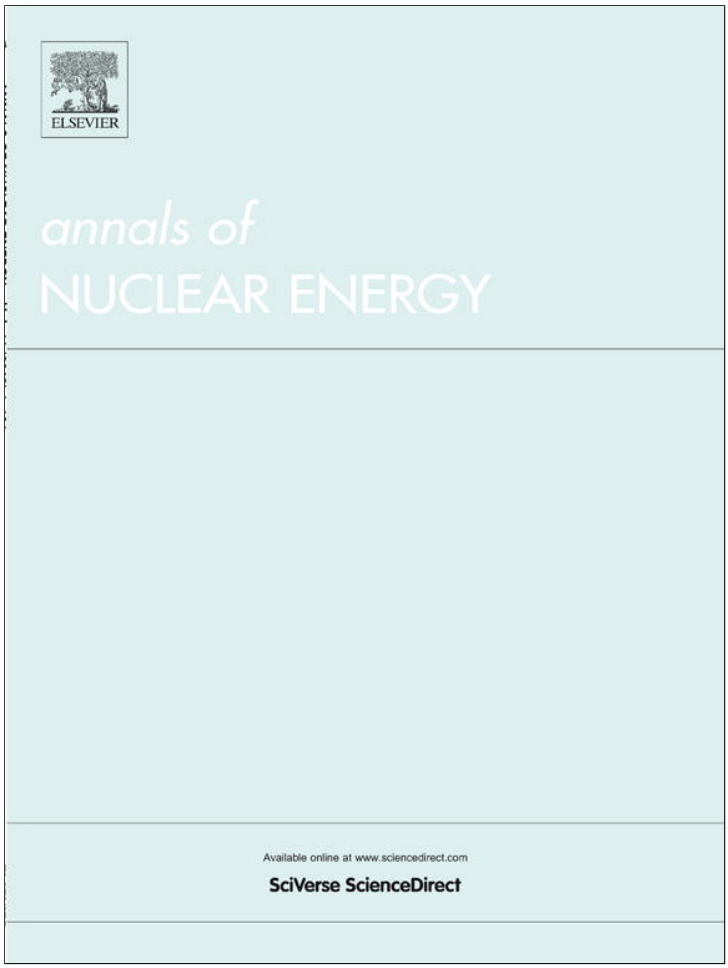

(This is a sample cover image for this issue. The actual cover is not yet available at this time.)

Annals of Nuclear Energy 51 (2013) 156–166

Contents lists available at SciVerse ScienceDirect

Annals of Nuclear Energy

journal homepage: www.elsevier.com/locate/anucene

Modeling and simulation of loss of the ultimate heat sink in a typical material testing reactor

Hisham El-Khatib [a], Salah El-Din El-Morshedy [a,*], Maher.G. Higazy [b], Karam El-Shazly [b]

[a] Atomic Energy Authority, Reactors Department, 13759 Cairo, Egypt
[b] Benha University, Department of Mechanical Power Engineering, Cairo, Egypt

ARTICLE INFO

Article history:
Received 2 May 2012
Received in revised form 27 July 2012
Accepted 30 July 2012

Keywords:
Thermal-hydraulics
Modeling and simulation
Loss of heat-sink
MTR

ABSTRACT

A thermal–hydraulic model has been developed to simulate loss of the ultimate heat sink in a typical material testing reactor (MTR). The model involves three interactively coupled sub-models for reactor core, heat exchanger and cooling tower. The model is validated against PARET code for steady-state operation and verified by the reactor operation records for transients. Then, the model is used to simulate the thermal–hydraulic behavior of the reactor under a loss of the ultimate heat sink event. The simulation is performed for two operation regimes: regime I representing 11 MW power and three cooling tower cells operated, and regime II representing 22 MW power and six cooling tower cells operated. In regime I, the simulation is performed for 1, 2 and 3 cooling tower cells failed while in regime II, it is performed for 1, 2, 3, 4, 5 and 6 cooling tower cells failed. The simulation is performed under protected conditions where the safety action called power reduction is triggered by reactor protection system to decrease the reactor power by 20% when the coolant inlet temperature to the core reaches 43 °C and scram is triggered if the core inlet temperature reaches 44 °C. The model results are analyzed and discussed.

1. Introduction

The research reactor safety calculations usually emphasize the simulations of the reactivity insertion accidents (RIA), and loss of flow accidents (LOFA). In the simulation of reactivity accidents it is customary to systematically consider transients with and without scram event, called respectively, protected transients and unprotected or self-limited transients, (Khater et al., 2007; Kazeminejad, 2006; Housiadas, 2002; El-Messiry, 2000; Mirza et al., 1998; Nasir et al., 1999). With the reactor shutdown system enabled, all LOFA simulations predict that clad temperature remains well below the clad melting point (El-Morshedy, 2011, 2002; Mairy et al., 2003; Bokhari and Mahmood, 2005). Unprotected LOFA is also investigated by (Hamidouche et al., 2004; Housiadas, 2000) where it is connected with the development of massive bulk boiling in the hot channel, inducing flow instabilities of the Ledinegg type. In the event of loss of heat sink, it is postulated the fault of parts of the secondary system, also it is considered the possibility of failure on the cooling towers of the main heat sink. The primary coolant system forced circulation is available and no coolant losses from the primary system. Little work has been done to investigate the loss of ultimate heat sink however it is considered as a design basis accident. Therefore, the objective of the present work is to develop a thermal–hydraulic model to simulate the behavior of a typical material testing reactor (MTR) reactor under loss of heat sink. The reactor under the present study (Khater et al., 2007; El-Morshedy, 2002) is a pool-type reactor with an open water surface and variable core arrangement. The core power is 22 MW, cooled by light water, moderated by water and with beryllium reflectors. It has a plate-type fuel elements with aluminum clad. Fig. 1 shows a schematic diagram for the reactor cooling systems. After reactor shutdown, decay heat is removed by natural circulation mechanism through flap valves. In order to reduce the irradiation level above the reactor pool due to the upward coolant flow direction in the reactor core, a prismatic structure, known as the chimney is mounted on the core grid, forming with its walls a vertical duct around the fuel elements with a lateral derivation opening that allows the passage of water from the core circuit towards the exit, a vast water column of 10 m above the core is adapted to act as radiation shielding, a small downwards flow was directed from above the reactor core in the upper part of the chimney in order to drag along any possibly active element. The ultimate heat sink consists mainly of six cells cooling tower, each cell has a cooling capacity of 4.1 MW. A summary of the key features of the reactor are shown in Table 1.

2. Mathematical model

The mathematical model consists of three sub-models namely; reactor core model, heat exchanger model and cooling tower model.

* Corresponding author. Tel.: +20 2 44800939.
E-mail address: s.e.elmorshedy@gmail.com (S.E. El-Morshedy).

0306-4549/$ - see front matter © 2012 Elsevier Ltd. All rights reserved.
http://dx.doi.org/10.1016/j.anucene.2012.07.031

Nomenclature

A	area, m^2
c_p	specific heat at constant pressure, J/kg °C
D_h	hydraulic diameter, m
e	extrapolated distance, m
h	enthalpy, J/kg
h_{fg}	latent heat of vaporization, J/kg
HTC	convective heat transfer coefficient, W/m^2 °C
K	thermal conductivity, W/m^2 °C
M	mass, kg
Nu	Nusselt number
PPF	power peaking factor
q	volumetric heat generation, W/m^3
Re	Reynolds number
T	temperature, °C
$\overline{T}$	mean temperature, °C
w	coolant mass flow rate, kg/s
W	average thermal power of the reactor, W
x	radial coordinate, m
z	axial coordinate, m
z_e	half extrapolated length, m
z_c	half active length, m

Greek letters

ϕ	heat flux, W/m^2
ω	humidity ratio

Subscripts

a	air
c	cold
c	coolant
cl	clad
cv	control volume
f	fuel
h	hot
H	heated
m	maximum
v	vapor
w	water

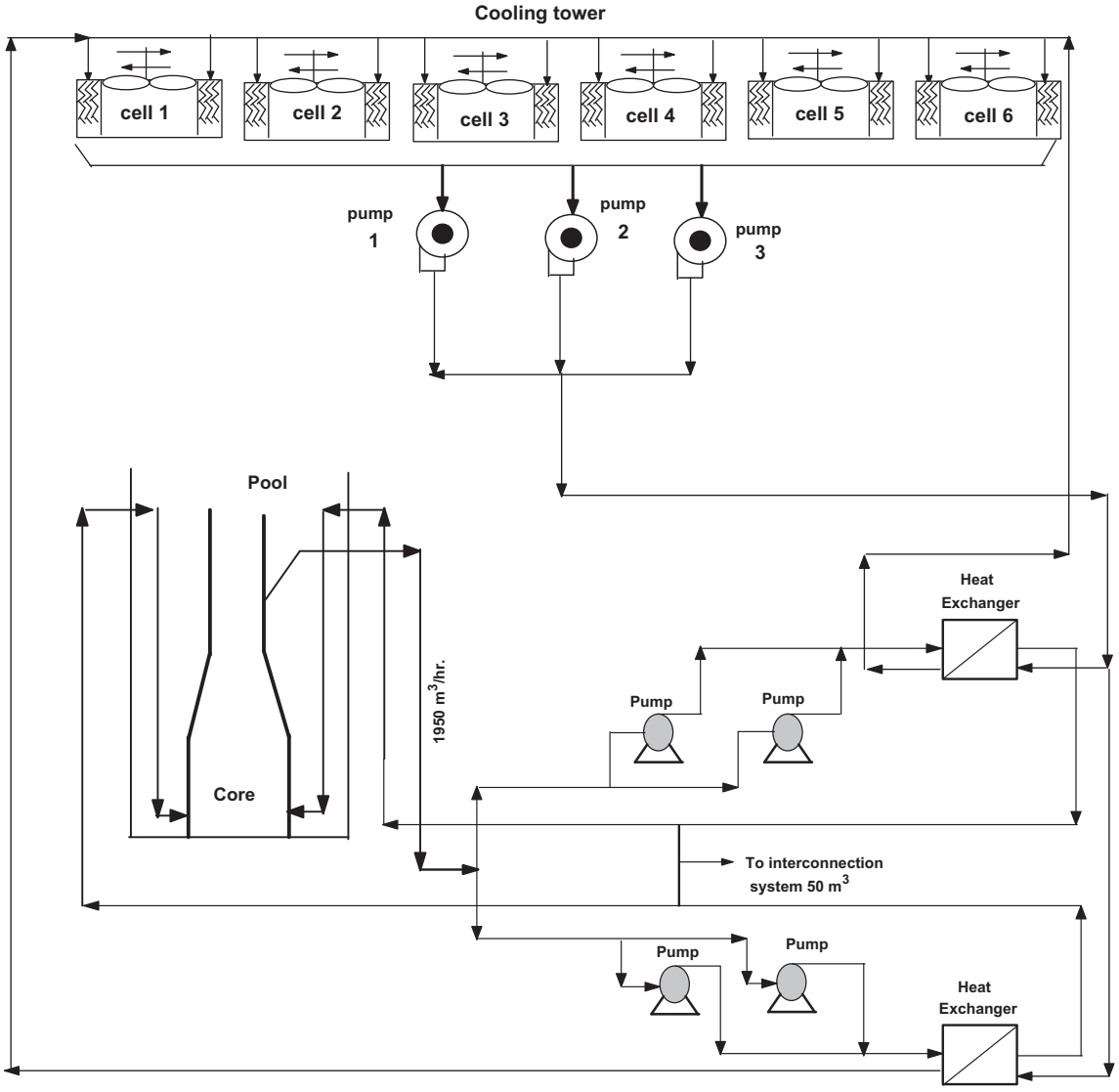

Fig. 1. Reactor core cooling systems.

Table 1
Reactor core design parameters [1].

Design thermal power (MW)	22
Water temperature at core inlet (°C)	40
Water temperature at core outlet (°C)	50
Nominal core flow (m^3/h)	1900
Number of fuel elements	29
Number of fuel plates per fuel element	19
Enrichment (%)	19.7
Total peaking factor	3.0
Axial peaking factor	1.35
Active length (cm)	80.0
Extrapolated length (cm)	8.0
External section of fuel element (cm^2)	8.0 × 8.0
Section in grid to house the FE (cm^2)	8.1 × 8.1
Plate thickness (cm)	0.15
Fuel thickness (cm)	0.07
Fuel width (cm)	6.40
Frame thickness (cm)	0.50
Frame width (cm)	8.0
External distance between frames (cm)	8.0
Internal distance between frames (cm)	7.0
Water gap between plates: of a single fuel element (cm) of different fuel elements (cm)	0.27 0.39
Upper plenum (cm)	12.0
Inlet channel length (cm)	15.0

2.1. Reactor core model

The core model includes the determination of coolant, clad and fuel temperatures in both steady and transient states. The coolant channel is divided into a specified axial regions while the fuel plate is divided into a specified radial nodes, then a nodal thermal–hydraulic calculation for both average and hot channels is performed with a chopped cosine heat generation flux. Fig. 2 shows a scheme of MTR fuel element with rectangular geometry.

2.1.1. Steady-state

2.1.1.1. Coolant temperature. It is assumed that the heat generated is transferred via convection from the fuel plate to the coolant, with no heat transmission via conduction existing in a lengthwise direction along the fuel plate. The amount of heat generated per unit time in an elemental volume of fuel core, situated at a distance z from the origin of the coordinates is:

$$dQ_g(z) = q(z) \cdot A_{th} \cdot dz \tag{1}$$

where A_{th} is the cross sectional area of the fuel and $q(z)$ is the local volumetric heat generation given by:

$$q(z) = q_m \cos\frac{\pi z}{2 \cdot z_e} \tag{2}$$

where q_m is the maximum volumetric heat generation (at the core center) and z_e is the extrapolated length, $z_e = z_c + 2e$, where z_c is half of the active length and e is the extrapolated distance.

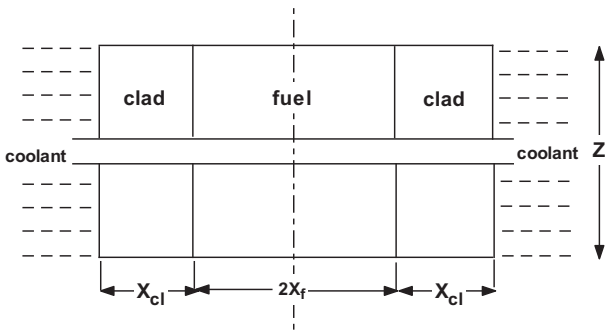

Fig. 2. Scheme of MTR fuel plate.

The amount of heat removed by the coolant per unit time is:

$$dQ_r(z) = w \cdot c_p \cdot dT \tag{3}$$

where w is the coolant mass flow rate.

At steady state, the amount of heat generated should be equal to the amount of heat removed,

$$dQ_g(z) = dQ_r(z) \tag{4}$$

Substituting from Eqs. (1)–(3) in Eq. (4):

$$dT = \frac{q_m \cdot A_{th}}{w \cdot c_p} \cdot \cos\frac{\pi \cdot z}{2 \cdot z_e} \cdot dz \tag{5}$$

By integrating both sides, we obtain the distribution function for the average temperature of the coolant in a lengthwise direction along the channel.

$$T_c(z) = T_i + \frac{q_m \cdot A_{th}}{w \cdot c_p} \cdot \frac{2 \cdot z_e}{\pi} \left[\sin\frac{\pi \cdot z}{2 \cdot z_e}\right]_{-z_c}^{z} \tag{6}$$

where T_i is the coolant inlet temperature.

2.1.1.2. Clad temperature. Clad-surface temperature is calculated by applying Newton's cooling law:

$$\phi(z) = HTC \cdot (T_{cl}(z) - T_c(z)) \tag{7}$$

where HTC is the local heat transfer coefficient.

$$\phi(z) = \phi_m \cdot \cos\frac{\pi z}{2 \cdot z_e} \tag{8}$$

where ϕ_m is the maximum admissible heat flux.

The clad-surface temperature is calculated as:

$$T_{cl}(z) = T_{cl,i}(z) + \frac{\phi(z)}{k_{cl}} x_{cl} \tag{9}$$

where $T_{cl,i}(z)$ is the inner clad-surface temperature and x_{cl} is the clad thickness.

2.1.1.3. Fuel temperature. The fuel temperature distribution is calculated by solving the general heat conduction equation for one dimension at steady-state condition:

$$\frac{d^2T_f}{dx^2} = -\frac{q(z)}{k_f} \tag{10}$$

With the boundary condition $dT/dx = 0$ at $x = 0$ and $T_f(z,x_f) = T_{cl,i}(z)$ where x_f is the half fuel thickness.

The fuel temperature is then determined as:

$$T_f(z,x) = \frac{q(z)}{2k_f}(x_f^2 - x^2) + T_{cl,i}(z) \tag{11}$$

2.1.2. Transient-state

The water coolant is considered incompressible in turbulent regime. A transient heat balance for the lumped, coolant, clad and fuel are as follows:

Coolant:

$$M_c c_{pc}\left(\frac{dT_c}{dt}\right) = -2w * c_{pc} * (T_c - T_i) = HTC * A_{cl}(T_{cl} - T_c) \tag{12}$$

Aluminum clad:

$$M_{cl} c_{pcl} \frac{dT_{cl}}{dt} = \frac{U(A_f + A_{cl})}{x_f + x_{cl}}[T_f - T_{cl}] - \frac{HTC * A_{cl}}{d}(T_{cl} - T_c) \tag{13}$$

Fuel interior:

$$M_f c_{pf} \frac{dT_f}{dt} = \phi_a * PPF * A_f - \frac{U(A_f + A_{cl})}{x_f + x_{cl}}[T_f - T_{cl}] \tag{14}$$

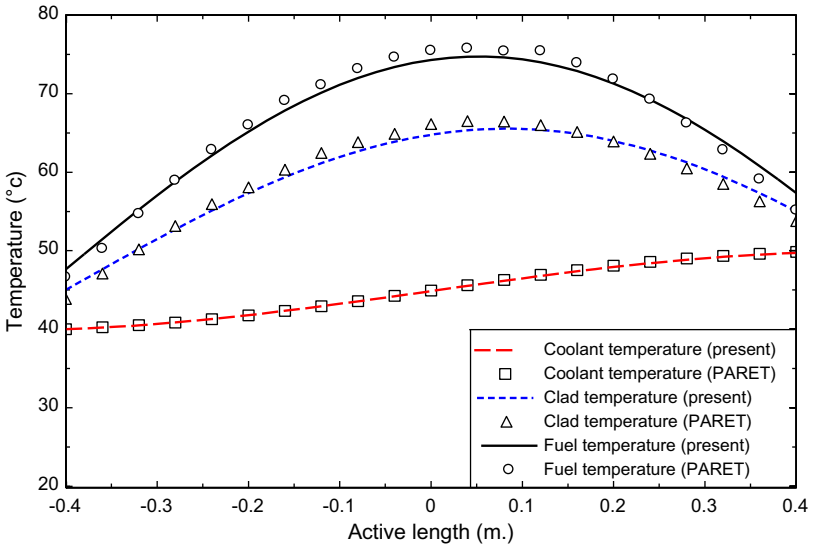

Fig. 3. Temperature distribution along the average channel.

where ϕ_a is the core average heat flux and U is the overall heat transfer coefficient given by $\frac{1}{U}=\frac{x_f}{k_f}+\frac{x_{cl}}{k_{cl}}$.

The mean value of an axially dependent temperature is given by

$$T(t)=\frac{1}{2z_c}\int_{-z_c}^{z_c}\overline{T}_c(z,t)dz \tag{15}$$

The axial temperature distributions of fuel, clad, and coolant in terms of the mean temperatures as follows [12]:

$$T_{cl}(z)=T_c(z)-(\overline{T}_{cl}-\overline{T}_c)\cos\left(\frac{\pi(z-(z_c/2))}{z_e}\right) \tag{16}$$

$$T_f=T_{cl}(z)+(\overline{T}_f-\overline{T}_{cl})\cos\left(\frac{\pi(z-(z_c/2))}{z_e}\right) \tag{17}$$

The axial position at which the maximum fuel and clad temperature occurs are

$$z_{\max}=\frac{z_c}{2}+\frac{z_e}{\pi}\tan^{-1}\frac{2}{\pi}\frac{z_e}{z_c}\frac{(\overline{T}_c-T_i)}{(\overline{T}_f-\overline{T}_c)} \tag{18}$$

The maximum coolant temperature is the outlet temperature T_{co}, where

$$T_{co}=2\overline{T}_c-T_i \tag{19}$$

where $\overline{T}$ is the mean temperature.

As the flow condition is always considered turbulent flow, the heat transfer coefficient, *HTC* is calculated by (Dittus and Boelter, 1930) equation:

$$Nu=0.0243Re^{0.8}Pr^{0.4} \tag{20}$$

2.2. Heat exchanger model

The heat exchangers used are of ALFA-LAFAL plate type consisting of 162 of corrugated plates. In the heat exchanger the primary coolant flows upward on one side of the plates and the secondary coolant flows downward on the other side. The secondary coolant system removes the heat from the primary system heat exchangers and transfers it to the environment through cooling tower units. The main heat exchanger data are shown in Table 2.

Both the hot and cold streams are assumed to be incompressible and average fluid properties are used. Consider a control volume of heat exchanger, and applying the energy conservation equation in dynamic state as follows (Massoud, 2002):

Table 2
Heat exchanger main data.

Number of plates	162
Heat transfer area (m^2)	294
Plates material	AISI316
Plate thickness (mm)	0.5
Primary side liquid volume (l)	504
Secondary side liquid volume (l)	510
Fluid relative direction	Counter flow
Active height (mm)	1842
Thermal capacity (MW)	11

Table 3
Cooling tower design parameters.

Parameter	Value
Number of cells	6
Water flow rate per cell (m^3/h)	520
Hot water temperature (°C)	37.0
Cold water temperature (°C)	30.0
Wet bulb temperature (°C)	24.0
Range (°C)	7.0
Approach (°C)	6.0
Fan speed (rpm)	380
Fan power (hp)	48.1
Water to air mass flow ratio (L/G)	1.366

$$Q_{i-1}-Q_i=\frac{\partial}{\partial t}(m_i c_{pw}T_i)$$

$$Q_{i-1}=w_{w,h}c_{pw}(T_{h,in}-T_{h,out})$$

$$Q_i=U*A*\Delta T_{LMTD}$$

$$M_{w,h}c_{pw}\frac{dT_{h,out}}{dt}=w_{w,h}c_{pw}(T_{h,in}-T_{h,out})-U\times A\times\Delta T_{LMTD} \tag{21}$$

$$M_{w,c}c_{pw}\frac{dT_{c,out}}{dt}=U\times A\times\Delta T_{\mathrm{LMTD}}-w_{w,h}c_{pw}(T_{c,out}-T_{c,in}) \tag{22}$$

where ΔT_{LMTD} is the logarithmic mean temperature difference given by:

$$\Delta T_{LMTD} = \frac{(T_{h,in} - T_{c,out}) - (T_{h,out} - T_{c,in})}{(\ln(T_{h,in} - T_{c,out})/(T_{h,out} - T_{c,in}))}$$

A finite difference approximation is utilized to simulate the above governing differential equations. The above differential equations are assumed to be initial value problem.

2.3. Cooling tower model

The conservation equation of energy for a control volume of the cooling tower is given by (Kröger, 2004; Donald Kern, 1980):

$$\frac{dh_w}{dt} + \left(\frac{1}{m_{cv}}\sum_1^n w_i\right)h_{out} = \frac{1}{M_{cv}}\sum_1^n w_{in}h_{in} \tag{23}$$

$$h_i = h_{air,in} + h_{w,in}$$

$$h_{out} = h_{air,out} + h_{w,out}$$

The enthalpy of the air–water vapor mixture per unit mass of dry air is expressed by:

$$h_{air,in} = c_{pa}T_{ai,in} + \omega(h_{fg} + c_{pv}T_{a,in})$$

$$\frac{dh_{w,out}}{dt} = \frac{1}{M_{cv}}(w_w h_{w,in} + w_{air}h_{air,in}) = \frac{1}{M_{cv}}(w_w h_{w,out} + w_{air}h_{air,out}) \tag{24}$$

Table 3 shows the main design parameters of the reactor cooling tower.

3. Model assessment

3.1. Steady-state

In steady-state normal operation, the model is validated against PARET (Obenchian, 1969) code. The temperature distributions along the axial direction are shown in Figs. 4 and 5 for average and hot channels respectively. The maximum coolant temperatures are achieved at the channel exit; their values are 50 °C and 62 °C for the average and hot channels respectively. The maximum

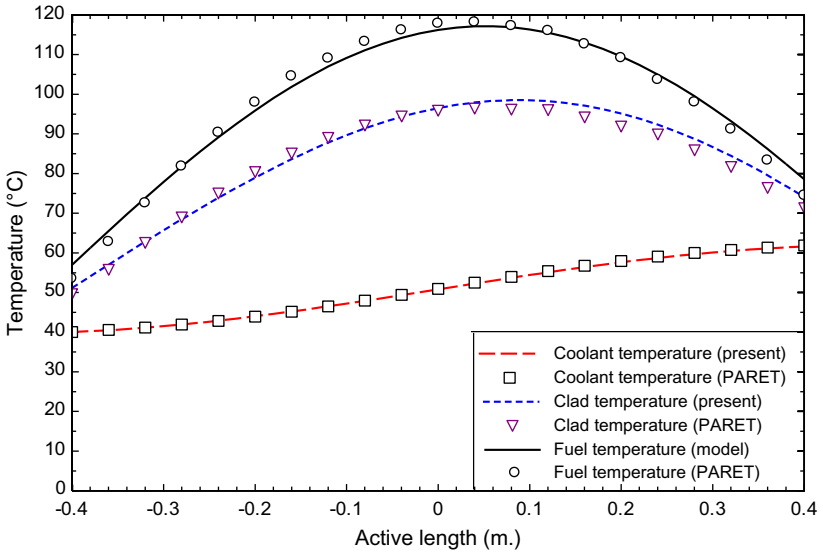

Fig. 4. Temperature distribution along the hot channel.

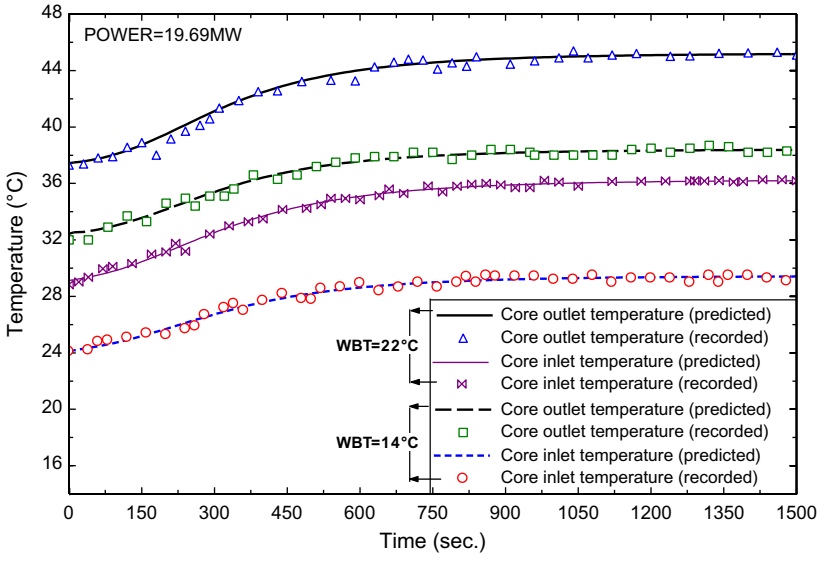

Fig. 5. Comparison between the predicted and recorded core inlet and outlet temperatures.

Table 4
Maximum temperature values predicted by the present model and PARET code.

Maximum temperatures	Average channel		Hot channel	
	Present	PARET	Present	PARET
Coolant	50.0	49.8	62.0	62.0
Clad-surface	65.0	66.5	95.5	96.4
Fuel-center	75.0	76.8	118.0	119.2

values of clad-surface and fuel-center temperatures are shifted from the channel center in the direction of flow. Table 4 shows the maximum temperature values predicted by the present model and PARET code for both the average and hot channels. Table 3 and Figs. 3 and 4 show a good agreement between the results of the present model and PARET code for steady-state operation.

3.2. Transient-state

In transient-state, the model is verified against the reactor operational data records at a power of 19.69 MW and two different ambient wet bulb temperatures of 14 °C and 22 °C during reactor operation period of 1500 s. Figs. 5 and 6 show comparisons between the predicted and recorded inlet and outlet temperatures for the reactor core and cooling tower respectively. The results show a good agreement between the predicted and recorded data.

4. Results and discussion

The present model is used to simulate the loss of the reactor ultimate heat sink. Simulation is performed for two operation regimes namely; regime I and regime II. In regime I, the reactor is operated at a power of 11 MW; only one primary cooling branch is used with one pump and one heat exchanger. In the secondary cooling system, three cooling tower cells with one operated pump are running. While in regime II, the reactor operates at a power of 22 MW, two primary cooling branches are operated with one pump and one heat exchanger in each branch, and six cooling tower cells with two operated pumps are running in the secondary cooling system. The simulation of the heat sink failure is performed by excluding cooling tower cells one by one respectively. The reac-

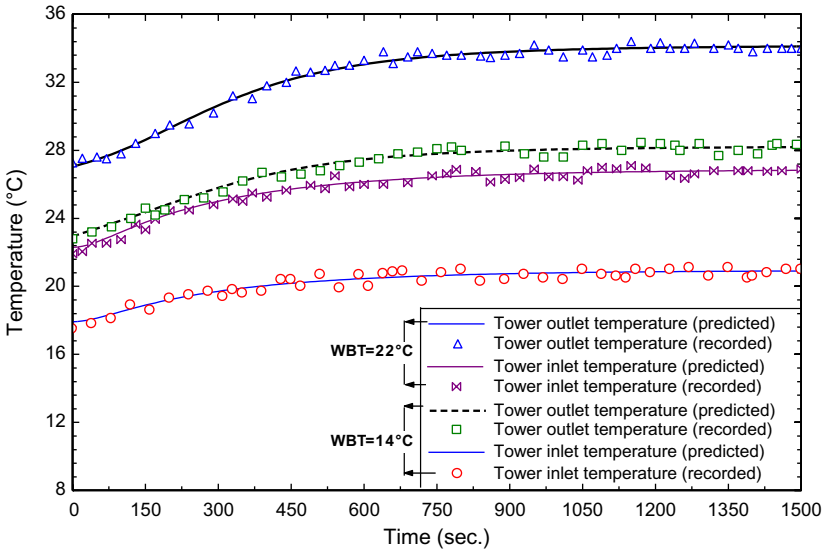

Fig. 6. Comparison between the predicted and recorded cooling tower inlet and outlet temperatures.

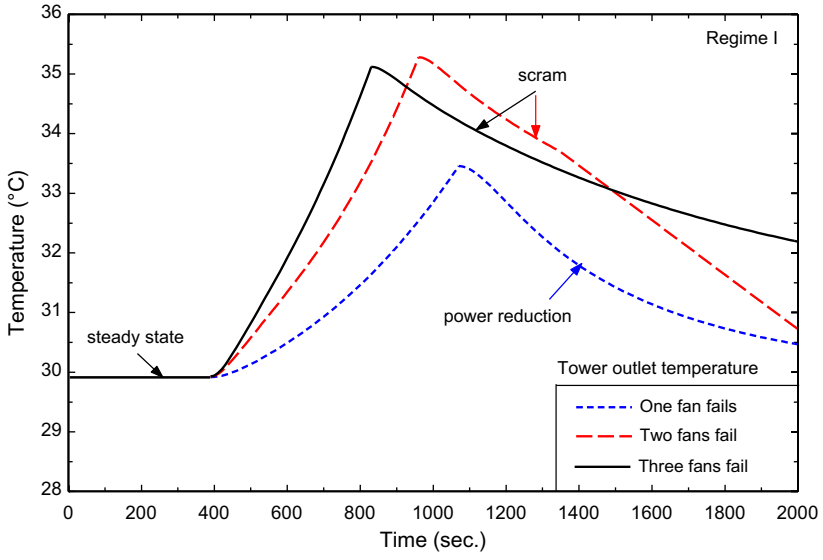

Fig. 7. Cooling tower outlet temperature variation during loss of heat sink for regime I.

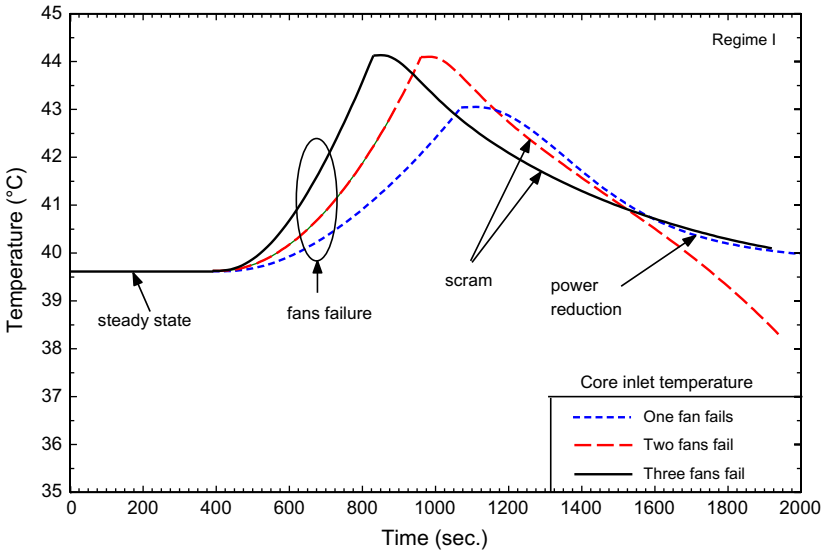

Fig. 8. Core inlet temperature variation during loss of heat sink for regime I.

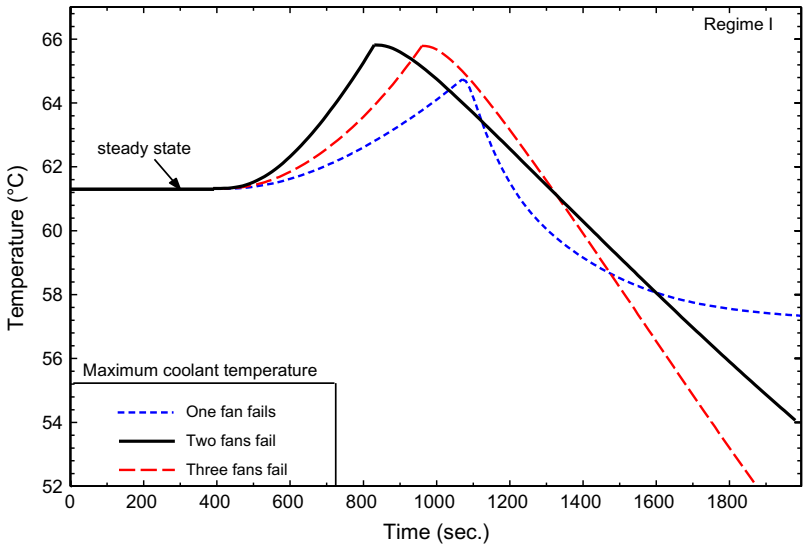

Fig. 9. Maximum coolant temperature variation during loss of heat sink for regime I.

tor is considered operating at its design parameters for steady-state normal operation before the loss of heat sink occurred. The reactor protection system is enabled during the simulation; therefore reactor power limitation to its eighty percent is triggered in case of reactor core inlet temperature reaching 43 °C. If the inlet temperature continues increasing to reach 44 °C, another safety action is recalled to shut down the reactor by scram.

The following events are considered in the simulation at regime I:

(1) One cooling tower cell fails.
(2) Two cooling tower cells fail.
(3) Three cooling tower cells fail.

It is assumed that, the reactor was operated at its nominal power (11 MW) for 400 s steady-state operation before the loss of heat sink initiated.

Fig. 7 shows the variation of the cooling tower outlet temperature during loss of the heat sink due to one, two and three cooling tower cells fail. The outlet temperature increased as fans excluded from the system, one failed fan leads to power reduction due to high core inlet temperature as described subsequently, and then the cooling tower outlet temperature reaches a maximum value of 33.7 °C at time of 1085 s. For cases of two and three fans fail, the reactor is scrammed and the maximum cooling tower outlet temperature reaches a value of 35.2 °C at times of 970 and 840 s for the two cases respectively. Fig. 8 shows the variation of the core inlet temperature during loss of the heat sink due to one, two and three cooling tower cells failure. The failure of one cell leads to a rapid increase in the core inlet temperature to reach the safety limit (43 °C) and so a power reduction action to 80% is triggered leading the temperature to decrease gradually. In cases of two and three cells fail, the limitation action at inlet temperature of 43 °C could not stop the temperature rise and the inlet temperature increased to 44 °C and so scram is triggered due to high core inlet temperature leading the temperature to decrease gradually. Figs. 9–11 show the variation of the maximum hot channel coolant, clad-surface and fuel-center temperatures respectively during loss of the heat sink due to one, two and three cooling tower cells fail. During steady-state, the maximum value of the coolant tempera-

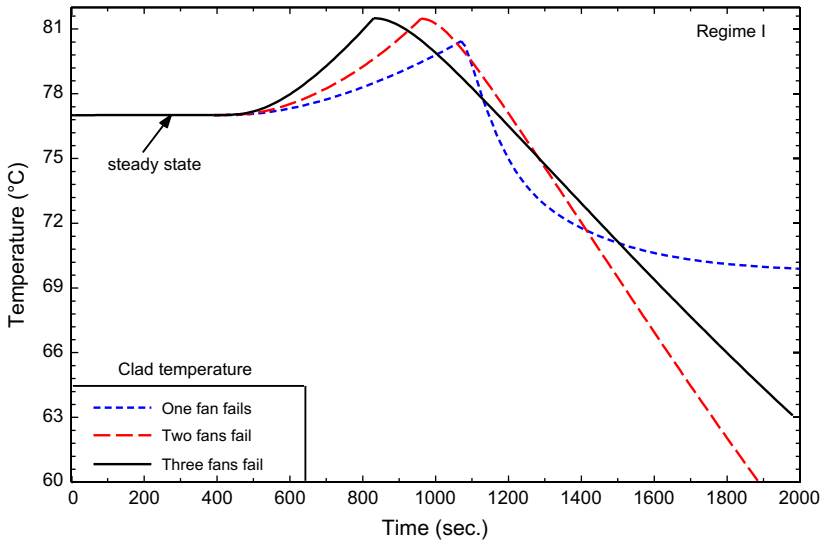

Fig. 10. Maximum clad-surface temperature variation during loss of heat sink for regime I.

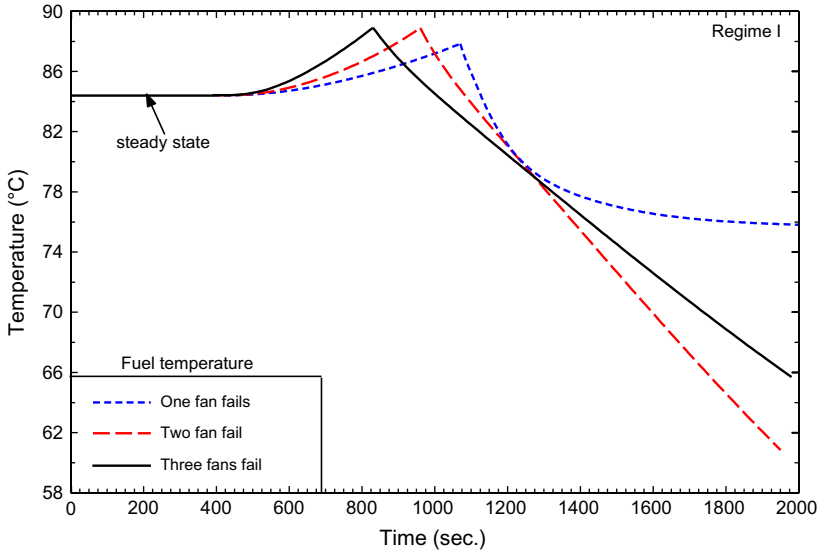

Fig. 11. Maximum fuel-center temperature variation during loss of heat sink for regime I.

ture in the hot channel is 62 °C at the channel exit. After the loss of one cooling tower cell, the core inlet temperature increased gradually and so the maximum coolant temperature in the hot channel increased gradually to reach 64.7 °C before limitation. For cases of two and three cooling tower cells fail, the maximum coolant temperature reaches 65.8 °C just before scram. Both the clad-surface and fuel-center temperatures follow the same trend with higher values. The maximum temperature values predicted and its occurrence time for regime I during the loss of heat sink events are depicted in Table 5. It shows that, the maximum coolant, clad-surface and fuel-center temperatures are far from the saturation, onset of nucleate boiling and blistering temperatures respectively.

The simulation of regime II includes the following events:

(1) One cooling tower cell fails.
(2) Two cooling tower cells fail.
(3) Three cooling tower cells fail.
(4) Four cooling tower cells fail.

Table 5
Maximum temperature values predicted during loss of heat sink for regime I.

Event	Coolant (°C)	Clad-surface (°C)	Fuel-center (°C)	Time (s)
One cell fails	64.7	80.4	87.8	1080
Two cells fail	65.8	81.5	88.9	970
Three cells fail	65.8	81.5	88.9	850

(5) Five cooling tower cells fail.
(6) Six cooling tower cells fail.

Fig. 12 shows the variation of the cooling tower outlet temperature during loss of the heat sink due to one, two, three, four, five and six cooling tower cells fail. The outlet temperature increased as fans excluded from the system, one failed fan leads to slight gradual increase in outlet temperature. While two fans fail lead to power reduction due to high core inlet temperature, and then

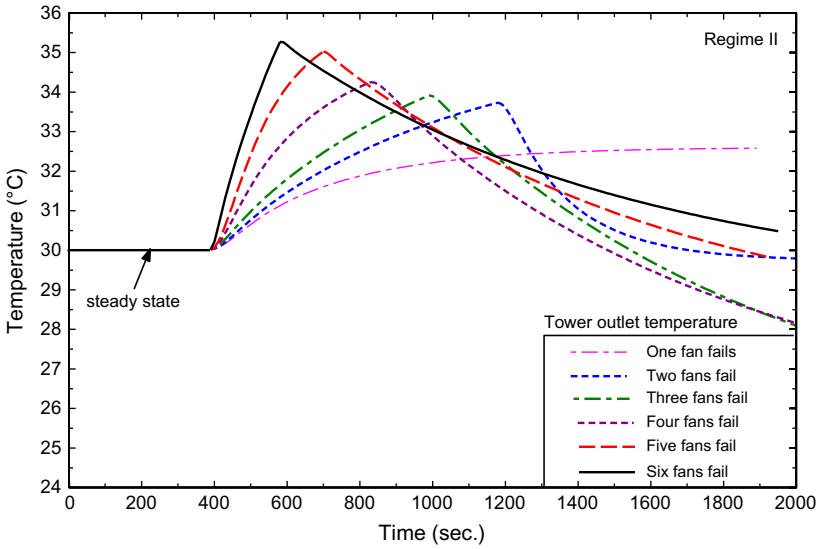

Fig. 12. Cooling tower outlet temperature variation during loss of heat sink for regime II.

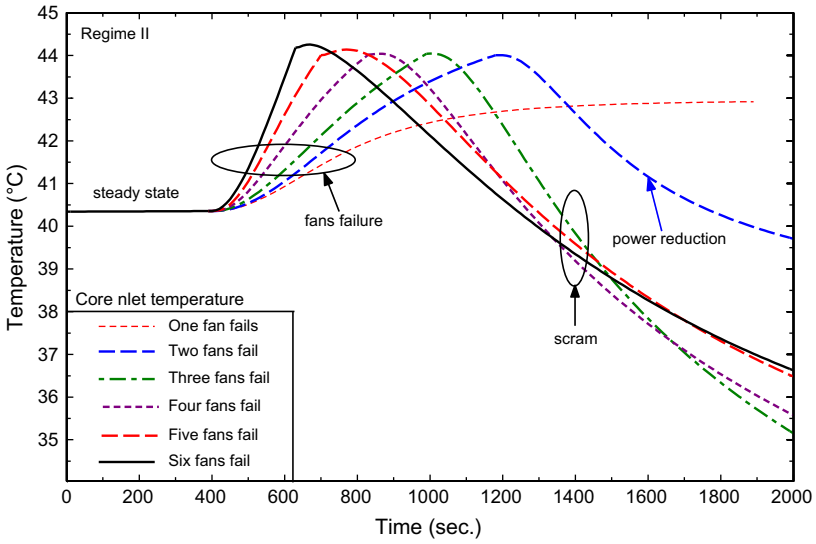

Fig. 13. Core inlet temperature variation during loss of heat sink for regime II.

the cooling tower outlet temperature reaches a maximum value of 32.92 °C at time of 940 s. The reactor is scrammed for cases of more than two cells fail and the maximum cooling tower outlet temperature reaches a value of 35.3 °C at times of 1000, 840, 710 and 640 s for the cases of three, four, five and six fans fail respectively. Fig. 13 shows the variation of the core inlet temperature during loss of the heat sink due to one, two, three, four, five and six cooling tower cells fail. The failure of one cell leads the core inlet temperature to increase gradually as the tower exit temperature increases to reach a maximum value of 42.6 °C by the end of the transient time which is still below the setting value. In case of two cells fail, the core inlet temperature increases more to reach the setting values (43 °C) and the power reduction is triggered at time of 780 s to reach 17.6 MW (80% the power before limitation) leading the core temperature to decrease rapidly. In case of more than two cooling tower cells fail, the core inlet temperature increases sharply and the power limitation action could not stop the temperature rise and so it reaches its highest limit (44 °C) and the reactor is scrammed leading the core inlet temperature to decrease rapidly.

Figs. 14–16 show the maximum coolant, clad-surface and fuel-center temperatures in the hot channel during loss of the heat sink due to one, two, three, four, five and six cooling tower cells fail. After the loss of one cooling tower cell, the core inlet temperature increased gradually and so the maximum coolant temperature in the hot channel also increased gradually from the steady-state value to reach 66.8 °C by the end of the transient time. In case of two cooling tower cells fail, the maximum coolant temperature reaches 67.5 °C before limitation and then decreased gradually. In case of more than two cells fail, the maximum coolant temperature increases to 68.6 °C before scram is triggered and then it decreases rapidly. The clad-surface and fuel-center temperatures follow the same trend of the coolant temperature within the same case but with higher temperature values and at different times depending on the scram time for each case. The maximum temperature values predicted and its occurrence time for regime II during the loss of heat sink events are depicted in Table 6. It also shows that, the maximum coolant, clad-surface and fuel-center temperatures are still faraway the saturation, onset of nucleate boiling and blistering temperatures respectively.

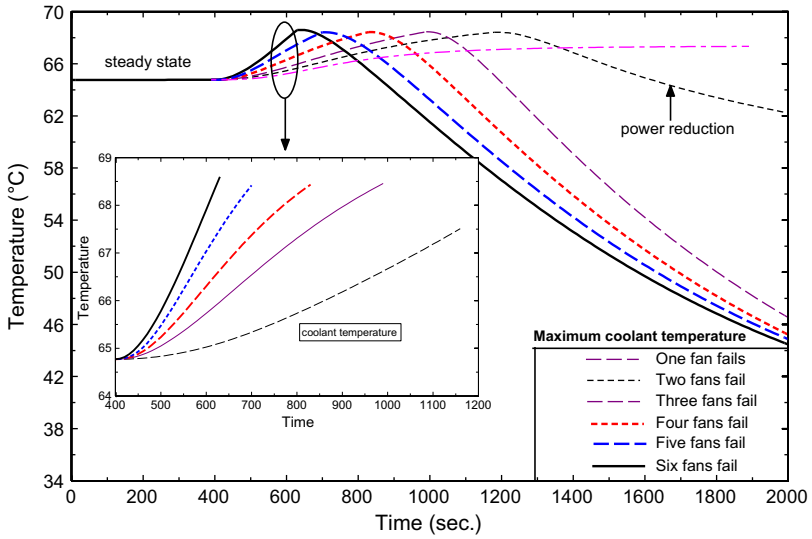

Fig. 14. Maximum coolant temperature variation during loss of heat sink for regime II.

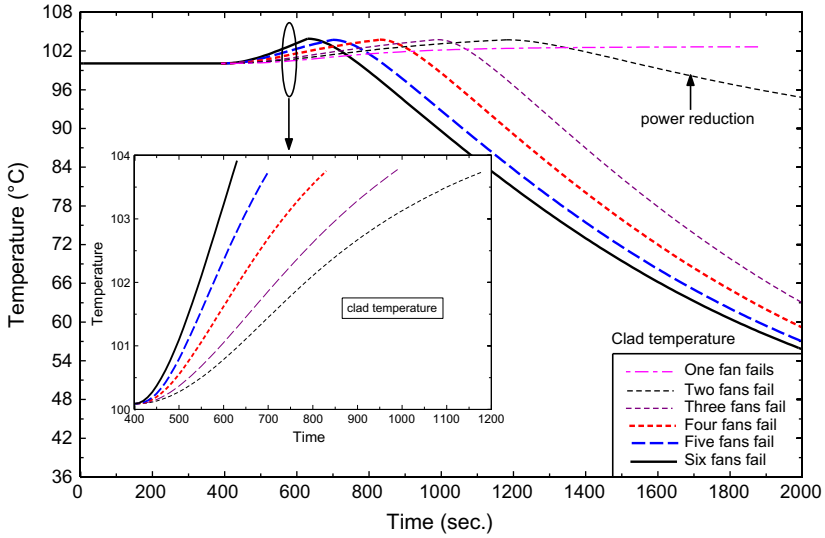

Fig. 15. Maximum clad-surface temperature variation during loss of heat sink for regime II.

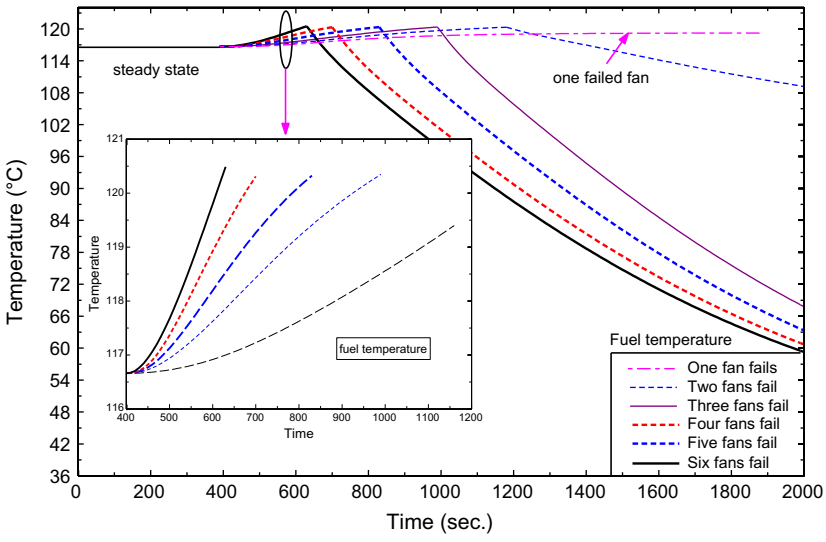

Fig. 16. Maximum fuel-center temperature variation during loss of heat sink for regime II.

Table 6
Maximum temperature values predicted during loss of heat sink for regime II.

Event	Coolant (°C)	Clad-surface (°C)	Fuel-center (°C)	Time (s)
One cell fails	66.8	102.6	119.2	1900
Two cells fail	67.5	102.8	119.9	930
Three cells fail	68.6	104.0	120.8	1000
Four cells fail	68.6	104.0	120.8	840
Five cell fail	68.6	104.0	120.8	710
Six cells fail	68.6	104.0	120.8	640

5. Conclusions

A thermal–hydraulic model is formulated for a typical MTR reactor using finite difference approximation of a group of differential equations that describe the reactor core, heat exchanger and cooling tower. The model includes both the primary and secondary cooling systems and predicts the fuel, clad, coolant temperatures in core as well as the inlet and outlet temperature of both the heat exchanger and cooling tower. The model is validated by PARET code for steady-state operation and verified also by the reactor operation records for transients. Then it is used to simulate the loss of the ultimate heat sink accident described by failure of cooling tower cells for two operation regimes. The first is for 11 MW power, one primary cooling branch and three cooling tower cells, while the second is for 22 MW power, two primary cooling branch and six cooling tower cells. The reactor protection system is enabled during the simulation. The model predicts power reduction safety actions and also scram taken by the reactor safety system to assure safe temperature levels, it is shown from the predicted results that, the maximum hot channel coolant, clad-surface and fuel-center temperatures achieved in the reactor has a satisfactory safety margin from saturation, onset of nucleate boiling and blistering temperatures respectively.

References

Bokhari, I.H., Mahmood, T., 2005. Analysis of loss of flow accident at Pakistan research reactor-1. Annals of Nuclear Energy 32, 1963–1968.

Dittus, F.W., Boelter, L.M.K., 1930. University of California, Berkeley, Publications on Engineering, vol. 2, p. 443.

Donald Kern, 1980. Process Heat Transfer. McGraw-Hill Book Company.

El-Messiry, A., 2000. Reactivity accidents analysis during natural core cooling operation of ETRR-2. Annals of Nuclear Energy 27, 1427–1439.

El-Morshedy, S.E., 2002. Transient Thermal Hydraulic Modeling for Off-Site Power Loss in Nuclear Reactors. PhD Thesis, Cairo University, Giza, Egypt.

El-Morshedy, S.E., 2011. Prediction, analysis and solution of the flow inversion phenomenon in a typical MTR-Reactor with upward core cooling. Nuclear Engineering and Design 241, 226–235.

Hamidouche, T., Salah, A.B., Adorni, M., D'Auria, F., 2004. Dynamic calculations of the IAEA safety MTR research reactor benchmark problem using RELAP5/3.2 code. Annals of Nuclear Energy 31, 1385–1402.

Housiadas, C., 2000. Simulation of loss of flow transients in research reactors. Annals of Nuclear Energy 27, 1683–1693.

Housiadas, C., 2002. Lumped parameter analysis of coupled kinetics and thermal-hydraulic for small reactor. Annals of Nuclear Energy 29, 1315–1325.

Kazeminejad, H., 2006. Reactivity insertion limits in a typical pool-type research reactor cooled by natural circulation. Annals of Nuclear Energy 33, 252–261.

Khater, H., Abu-El-Maty, T., El-Morshedy, S.E., 2007. Thermal-hydraulic modeling of reactivity accident in MTR reactors. Annals of Nuclear Energy 34, 732–742.

Kröger, D.G., 2004. Air-Cooled Heat Exchangers and Cooling Towers. PennWell Corp., Tulsa, Oklahoma.

Mariy, A., El-Morshedy, S.E., Khater, H., Abdel-Raouf, A., 2003. Transient thermal-hydraulic modeling of ETRR-2 for off-site power loss. IAEA-CN-100/64, International Conference on Research Reactor Utilization, Safety, Decommissioning, Fuel and Waste Management, Santiago, Chile, 10–14 November 2003.

Massoud, M., 2002. Engineering Thermo-fluids, Thermodynamics, Fluid Mechanics, and Heat Transfer. ISBN 10 3-540-22292-8. Springer, Berlin, Heidelberg, New York.

Mirza, A.M., Khanam, S., Mirza, N.M., 1998. Simulation of reactivity transients in current MTRs. Annals of Nuclear Energy 25, 1465–1484.

Nasir, R., Mirza, N.M., Mirza, S.M., 1999. Sensitivity of reactivity insertion limits with respect to safety parameters in a typical MTR. Annals of Nuclear Energy 26, 1517–1535.

Obenchian, C.F., 1969. PARET – A Program for the Analysis of Reactor Transients. Idaho National Engineering Laboratory, Report IDO-17282.